Activity of Antimicrobial Peptide Aggregates Decreases with Increased Cell Membrane Embedding Free Energy Cost

Rongfeng Zou[†,#], Xiaomin Zhu[†], Yaoquan Tu*[,#] , Junchen Wu*[,†,§] and Markita P. Landry*[,§,¶,α]

[†]Key Laboratory for Advanced Materials & Institute of Fine Chemicals, School of Chemistry and Molecular Engineering, East China University of Science and Technology, Shanghai 200237, China E-mail: jcwu@ecust.edu.cn

[#]Division of Theoretical Chemistry and Biology, School of Biotechnology, KTH Royal Institute of Technology, SE-10691 Stockholm, Sweden E-mail:yaoquan@kth.se

[§]Department of Chemical and Biomolecular Engineering, University of California Berkeley, 476 Stanley Hall, Berkeley, USA E-mail: landry@berkeley.edu

[α]Chan-Zuckerberg Biohub, San Francisco, CA

[¶]California Institute for Quantitative Biosciences (qb3), University of California-Berkeley, Berkeley, USA

CONTENT

S1 Unbiased MD simulations

All simulations were performed with GROMACS. CHARMM-36 force field was applied in the simulation. Force field parameters of guanine (PNA) were taken from the CHARMM-additive force field and converted to the GROMACS format. All covalent bonds were constrained to their equilibrium values using the LINCS algorithm. The electrostatic interactions were calculated by the Particle Mesh Ewald algorithm, and a cutoff of 1.0 nm was used both for Lennard – Jones interactions and for the real-space coulomb contributions. All the MGNs were energy-minimized and a short production run (1 ns) was performed with the NPT ensemble (T = 300 K, P = 1 atm). The minimized structures were subsequently used as starting structures for further simulation. In each system, we placed 4 peptides in the simulation box. After being solvated, 0.15M NaCl was added to the system to resemble a biological environment. Each box contains ca. 18500 TIP3P waters. Next, the systems were minimized and heated to 400 K for 200 ps constraining the heavy atoms (atoms other than hydrogens of the peptides) using a harmonic potential with force constant of 1000 kJ mol^{-1} nm^{-2}. We then equilibrated the system in the isobaric –isothermal ensemble (T = 400 K, P = 1 atm) for 400 ps with constrains on the backbone using the same harmonic potential used in the NVT. The constraint was used in the NVT and NPT equilibration process to avoid collapse of the simulation system. The final production runs were performed under the NVT ensemble (T = 400 K) for 2 μs without any constrains on the atoms.

The aggregation free energy landscape was plotted with the Rg of guanine units and the solvent accessible surface area (SASA) of peptides according to the following equation (1):

$$\Delta G = -k_B T \ln\left(\frac{p_x}{p_0}\right) \qquad (1)$$

where k_B is the Boltzmann constant, T is temperature, p_0 is the probability of the lowest energy state and p_x is the probability of state x.

SASA and Rg were calculated with the Gromacs tools (gmx sasa and gmx gyrate, respectively). Note that different MGNs have different numbers of guanine units, which can have different values in Rg. However, the distribution of Rg reflect the compactness of the guanine core.

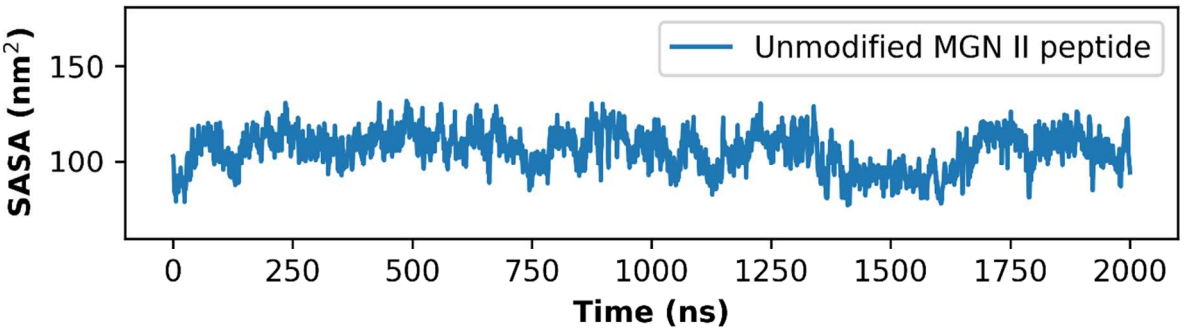

Figure S1. SASA time evolution of the unmodified MGN II peptide. Large fluctuation of SASA suggests that MGN II peptide can not form stable aggregates in solution, in good agreement with previous studies.[1, 2]

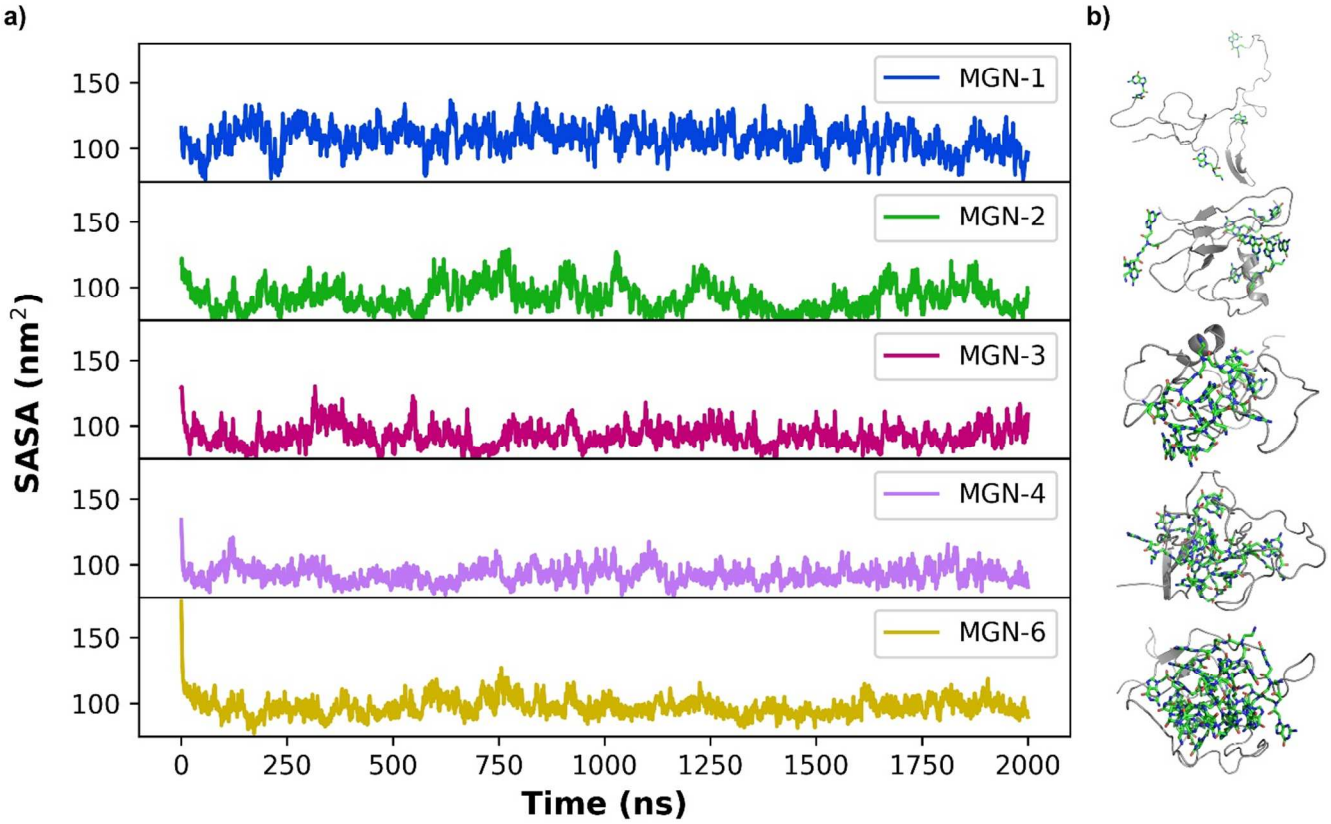

Figure S2. a) Time evolution of SASA of MGNs and b) the final structures with the highest probability for each MGNs (from top to bottom: MGN-1 to MGN-6). The guanine units are shown as sticks.

S2 Experimental material and instruments

All solvents were dried and distilled before use. Anhydrous dichloromethane (DCM) and dimethyl formamide (DMF) were distilled over $CaCl_2$ and CaH_2 respectively, and kept anhydrous with 4Å molecular sieves. N,N-Diisopropylcabodiimide (DIC), N,N-Diisopropylethylamine (DIEA) and Benzotriazol-1-yl-oxytripyrrolidinophosphonium hexafluorophosphate (PyBOP) were purchased from Suzhou Highfine Biotech Co., Ltd., Fmoc-PNA-G(Bhoc)-OH was purchased from Luoyang Chenglin Bio-tech Co., Ltd., Fmoc-protected amino acids were purchased from GL Biochem Ltd.

Analytical High Performance Liquid Chromatography (HPLC) was performed with the following parameters: reversed phase, (RP-C18) HPLC column (5 μm particle size) and UV detector. The mobile phase was a gradient of 5-100% of methanol aqueous solution containing 0.5% TFA at a total flow rate of 16 mL/min. The UV absorption peaked at 220 nm and 254 nm was recorded for analysis. All mass spectra were recorded with an M-TOF AB Sciex spectrometer. Analytical High Performance Liquid Chromatography (HPLC) was performed with the reversed phase C18.

S3 General synthesis of peptides

Fmoc Removal: The Fmoc protecting group was initially cleaved by treatment with 20% piperidine in DMF (10 mL) under microwave radio conditions (25 W, 50 ± 5 °C, 5 min). Next, the resin was washed 6×10 mL with DMF to

remove any traces of piperidine. A positive Kaiser test confirmed the cleavage of the Fmoc group and the formation of the free amine.

Standard Fmoc solid phase peptide synthesis techniques (SPPS): Each peptide was attached using Rink-amide resin (0.25 mmol) under microwave radio (35 W, 60±5°C, 20 min). Next, the resin was washed 7×20 mL with DMF to remove any remaining traces of amino acid. A negative Kaiser test confirmed the attachment of the amino acid.

Cleavage from the Resin: Cleavage of the product from the resin was achieved by treatment with a mixture of TFA/H_2O/triisopropylsilane (95:2.5:2.5) for 3 h. The cleavage mixture was collected by filtration and the resin was washed twice with pure TFA (8 mL). The filtrates were combined and concentrated under vacuum to recover an oily residue. The peptide was precipitated by adding dry diethyl ether to the oil, and collected with centrifugation. The solid was dissolved in water and lyophilized. Purity of the peptides was checked by HPLC on a RP18-column using water/MeOH (with 0.05% TFA) as the eluent. If necessary, crude peptides were purified by RP18-MPLC using the same conditions.

The starting Fmoc-based amino acids were used: Fmoc-Asn(Trt)-OH, Fmoc-Met-OH, Fmoc-Ile-OH, Fmoc-Glu(OtBu)-OH, Fmoc-Gly-OH, Fmoc-Val-OH, Fmoc-Phe-OH, Fmoc-Lys(Boc)-OH, Fmoc-Ala-OH, Fmoc-Ser(tBu)-OH, Fmoc-His(Trt)-OH, Fmoc-Trp(Trt)-OH, Fmoc-Leu-OH.

S4 Synthesis procedure

Rink Amide resin (510 mg, 0.25 mmol, 1 equiv.) was weighed and allowed to swell in DCM/DMF (5.0/5.0 mL) for 1.5 h. Next, the Fmoc protection group was removed under microwave radio conditions. After an intensive cycle with DMF, the following amino acids were attached under microwave radio conditions for SPPS: Fmoc-protected amino acid (0.75 mmol, 3 equiv), PyBOP (0.75 mmol, 3 equiv) and DIEA (2 mmol, 8 equiv) in DMF (15 mL). Then, the product was transferred into a glass peptide synthesis vessel, washed 1×30 mL with DCM, and 2×30 mL with DMF. Fmoc-PNA-G(Bhoc)-OH was attached at room temperature. The final product was cleaved from the solid support according to the general procedure for the Rink Amide Resin. The recovered product was a white solid as described in Table S**1-10.**

Table S1. Synthesis and analysis of MGN-1.

MGN-1**:** Yield 12.0%, purity HPLC 97.8%, MALDI-TOF (m/z): calcd for 2755.45, found $[M+H]^+$ 2756.23.
Guanine-GIGKFLHSAKKFGKAFVGEIMNS-NH_2

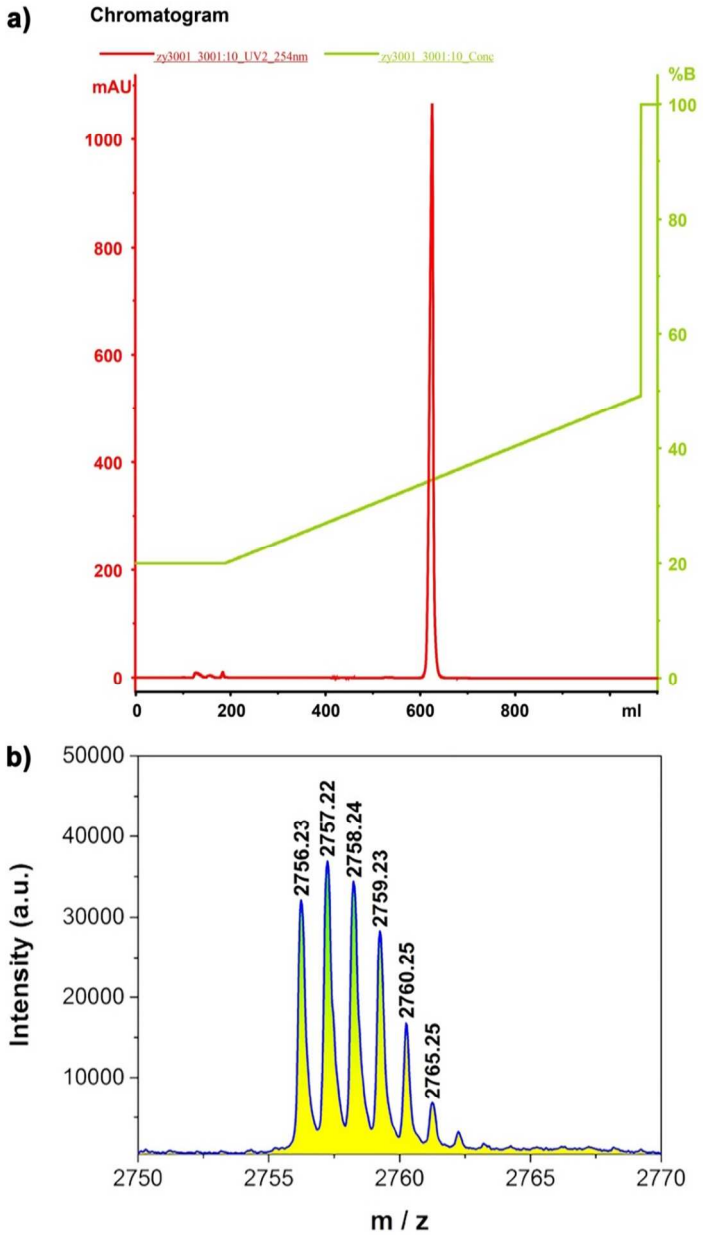

Figure S3. (a) HPLC analysis report and (b) M-TOF of MGN-1.

Table S2. The synthesis and analysis of MGN-2.

MGN-2: Yield 8.4%, purity HPLC 96.5%, MALDI-TOF (m/z): calcd for 3046.56, found $[M+H]^+$ 3047.54.
Guanine Guanine- GIGKFLHSAKKFGKAFVGEIMNS-NH_2

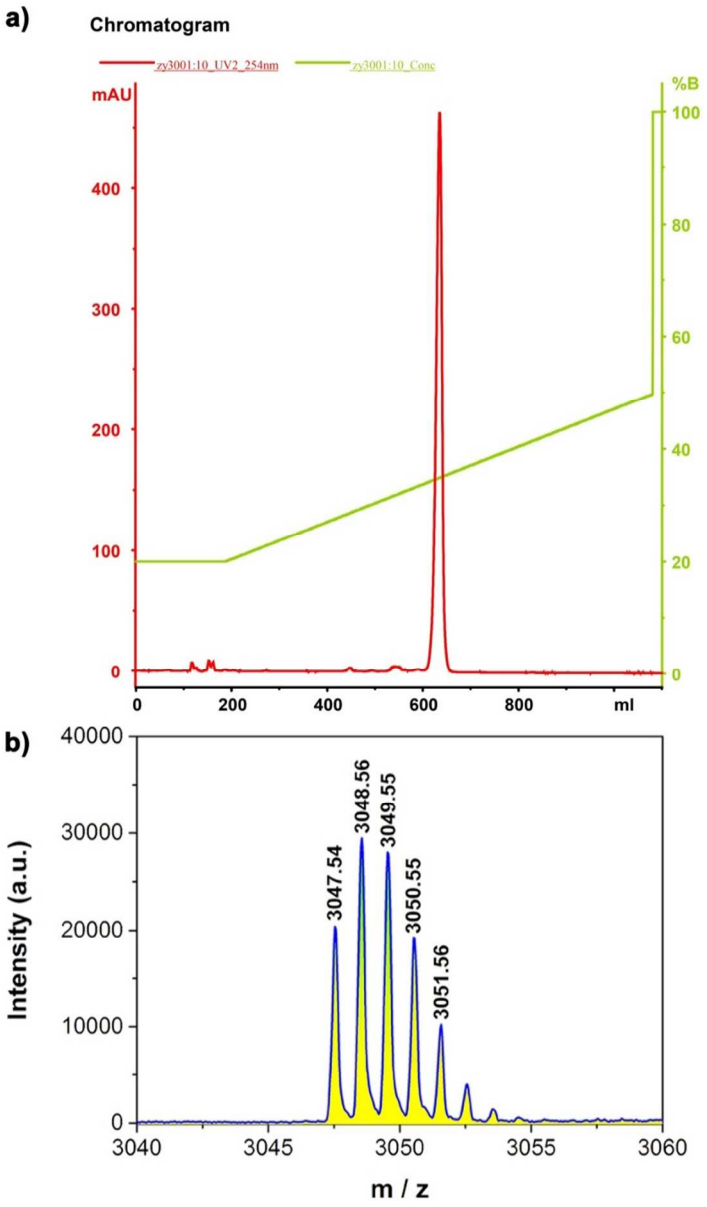

Figure S4. (a) HPLC analysis report and (b) M-TOF of MGN-2.

Table S3. The synthesis and analysis of MGN-3.

MGN-3: Yield 5.2%, purity HPLC 99.2%, MALDI-TOF (m/z): calcd for 3337.67, found $[M+H]^+$ 3338.57.
Guanine Guanine Guanine- GIGKFLHSAKKFGKAFVGEIMNS-NH_2

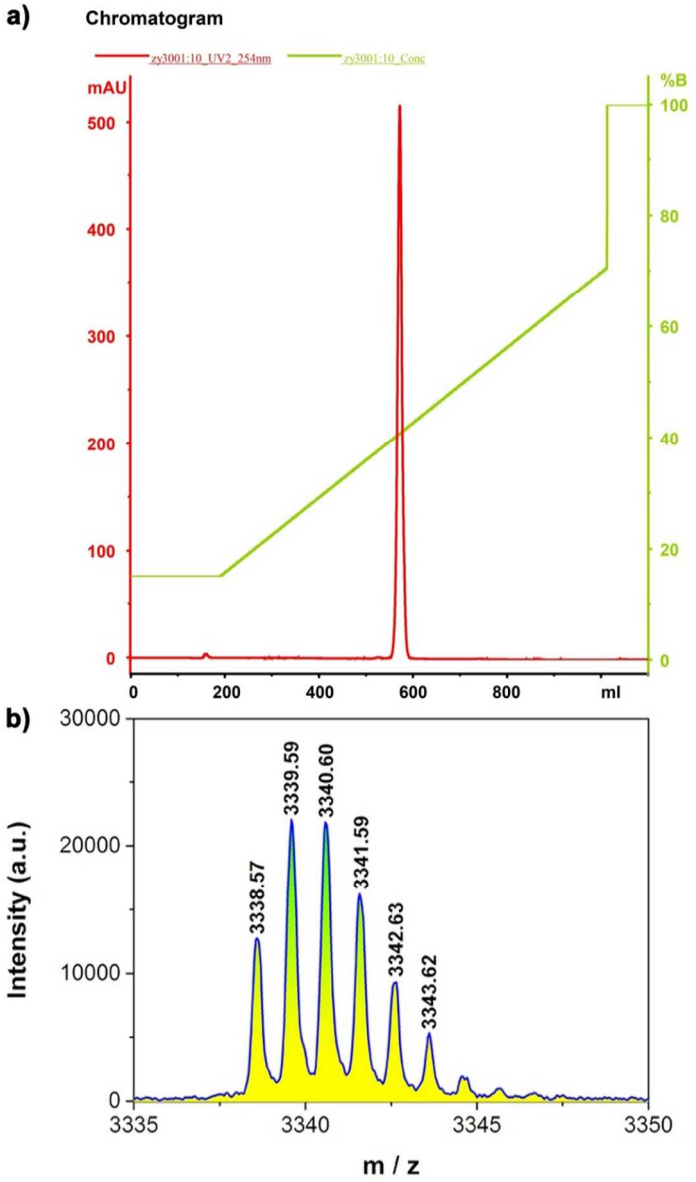

Figure S5. (a) HPLC analysis report and (b) M-TOF of MGN-3.

Table S4. The synthesis and analysis of MGN-4.

MGN-4: Yield 4.8%, purity HPLC 99.0%, MALDI-TOF (m/z): calcd for 3628.77, found $[M+H]^+$ 3629.88.
Guanine Guanine Guanine Guanine- GIGKFLHSAKKFGKAFVGEIMNS-NH_2

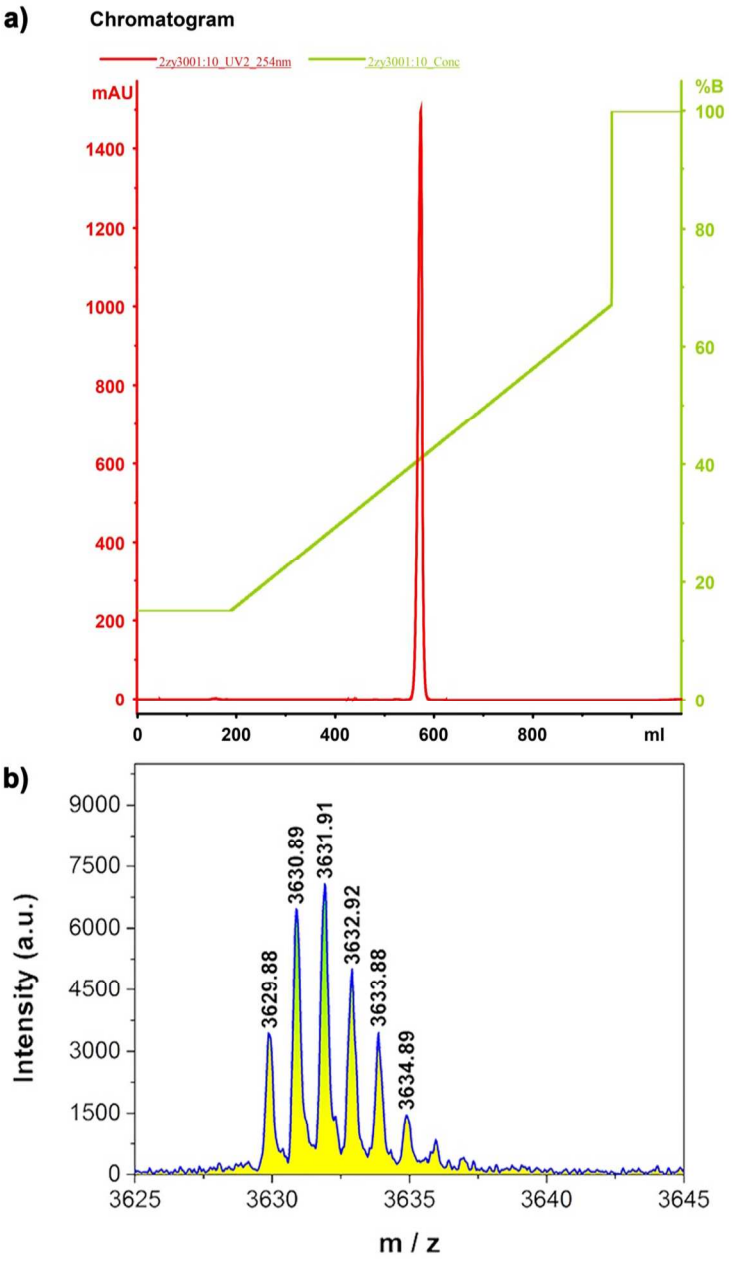

Figure S6. (a) HPLC analysis report and (b) M-TOF of peptide 4.

Table S5. The synthesis and analysis of MGN-6.

MGN-6: Yield 4.6%, purity HPLC 97.2%, MALDI-TOF (m/z): calcd for 4210.99, found $[M+H]^+$ 4211.93.
Guanine Guanine Guanine Guanine Guanine Guanine- GIGKFLHSAKKFGKAFVGEIMNS-NH_2

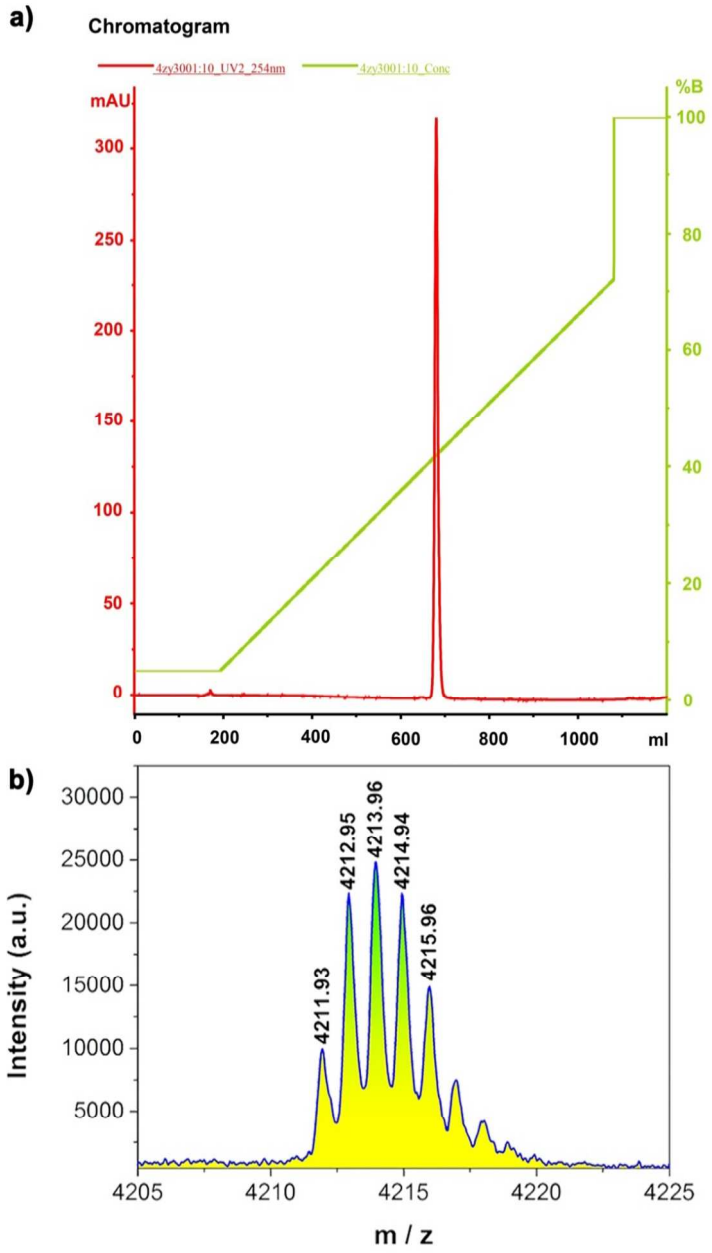

Figure S7. (a) HPLC analysis report and (b) M-TOF of MGN-6.

S5 Circular Dichroism (CD) of MGN 1-6

CD spectral measurements were performed using a Chira scan CD spectrometer (Applied Photophysics) with 2.0 mm path-length cell to scan. The wavelength range scanned was set from 200 to 320 nm, with 0.2s integration time, 1 nm step resolution, and 1 nm bandwidth. The concentration of each of the five peptides was 40 μM. Peptides MGN 1-6 were measured in triplicate in a Tris-buffer solution (TBS,10 mM Tris, pH 7.4, 25 °C), and then averaged. Background spectra of the solvents/buffer were acquired and subtracted from the sample spectra.

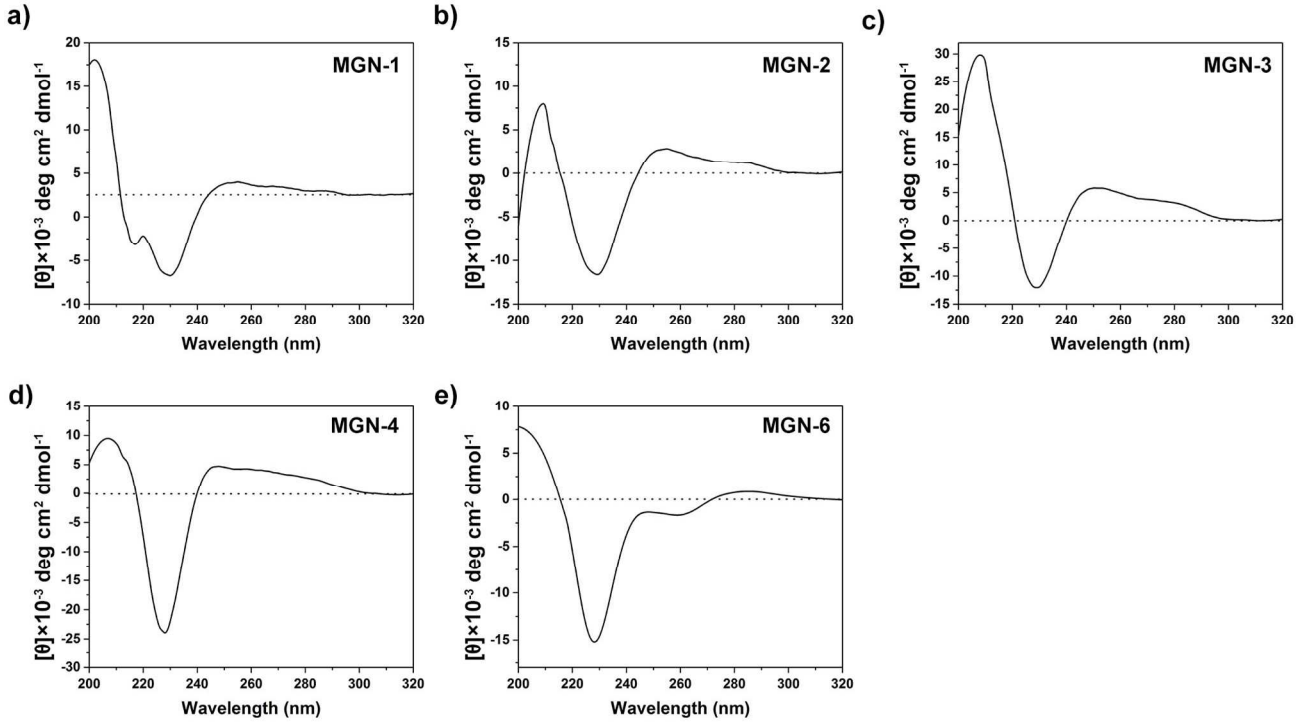

Figure S8. CD Spectra of MGNs 1-6 in TBS

S6 Antibacterial Assay

Three gram-negative bacteria (*Escherichia coli ATCC-25922, Acinetobacter ATCC-19606 and Citrobacter freundii ATCC-13316*) were used in this assay. Bacterial cells were inoculated and cultured at 37°C for 5 h in broth medium and then suspended in broth medium at 1~2 × 10^6 cells/mL to generate the working suspension. Different concentrations of peptides were prepared in a 96-well plate using broth medium, where each well contained 100 µL of the compound solution. 100 µL of the cell working suspension was added to each well. The plate was incubated at 37 °C for 24 h, and the optical density (OD) of each well was then measured at 600 nm after a gentle shaking of the plate for 10 sec using a Hybrid Multi-Mode Microplate reader (BioTek, Synergy H4). Wells containing medium only (blank) and wells containing cells in medium without peptides (positive control) were included on the same plate. The percentage of cell growth in each well was calculated from Bacteria Growth (%) = [(A_P – A_B)/(A_C – A_B)] × 100), where A_P is the mean absorbance value for a known peptide concentration, A_C is the mean absorbance value for the positive control, and A_B is the mean absorbance value for blank, plotted against peptide concentration to give the dose-response curves of antibacterial activity for these peptides. MIC_{50} is the minimum concentration which gave 50% inhibition to bacterial growth.

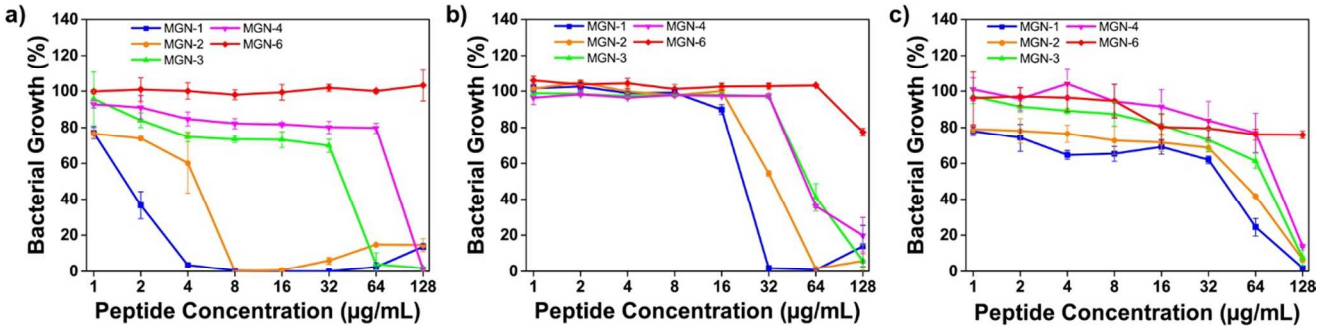

Figure S9. a) *E. coil*, b) *A. baumanmii* and c) *C. freundii* growth inhibition dose-response data for MGNs 1-6. Data was collected after the cell cultures were incubated for 8 h at 37 °C.

S7 Confocal laser-scanning microscopy (GLSM) images

Bacterial cells (*E. coli*) were inoculated and cultured in nutrient broth medium with shaking at 37 °C for 5 h and suspended in nutrient broth medium at a density of 1×10^6 CFU/mL for use. Next, bacteria were incubated with MGN-1 and MGN-6 at 37 °C for 1 h in nutrient broth medium at a concentration of 2.2 μg/mL (1.0 μM, MIC_{50} of MGN-1) for MGN-1, and 128 μg/mL (30.4 μM, the maximum concentration tested of MGN-6) for MGN-6, respectively, while the control group contained bacteria only. After incubation, centrifugation (7500 rpm, 5 min) was carried out and the supernatant was removed. LIVE/DEAD BacLight™ Bacterial Viability Kits (L13152) were used to stain bacteria at room temperature in the dark for 15 minutes. After 15 min, the bacteria were washed three times with PBS, suspended in pure water, placed (2 μL) onto the microscope slide, and dried at room temperature. CLSM images were acquired with a Nikon AIR confocal laser-scanning microscope and a 60-oil-immersion objective lens. Molecular Probes' LIVE/DEAD® BacLight™ Bacterial Viability Kits provide a two-color fluorescence assay of bacterial viability that has proven useful for a diverse array of bacterial genera. The Live/Dead BacLight Bacterial Viability Kits utilize mixtures of SYTO 9 green-fluorescent nucleic acid stain, a red-fluorescent nucleic acid stain, and a propidium iodide (PI) stain. These stains differ both in their spectral characteristics and in their ability to penetrate healthy bacterial cells. When used alone, the SYTO-9 stain generally labels all bacteria in a population: those with intact membranes along with those with damaged membranes. In contrast, PI penetrates only bacteria with damaged membranes, causing a reduction in the SYTO-9 stain fluorescence when both dyes are present. Thus, with an appropriate mixture of the SYTO-9 and PI stains, bacteria with intact cell membranes stain fluorescent green, whereas bacteria with damaged membranes stain fluorescent red. For SYTO-9, the light source at 488 nm provided excitation, and emission was collected at 500-550 nm; For PI, the light source at 561 nm provided excitation, and emission was collected at 570-620 nm.

S8 SMD/umbrella sampling simulation

Free energies of the guanine-tagged MGNs permeating into membrane were calculated by the umbrella sampling method. The membrane in the simulation was generated with the charmm-gui server (http://www.charmm-gui.org/)[3] and equilibrated. The membrane contains 192 1-palmitoyl-2-oleoyl-sn-glycero-3-phosphoethanolamine (POPE) and 64 2-oleoyl-1-pamlitoyl-sn-glyecro-3-glycerol (POPG) molecules, which are used to mimic the Gram-negative bacterial membrane. Next, the aggregate was put above the membrane and solvated with TIP3P water, followed with a 50000-step energy minimization to remove any bad contacts. The system was then heated to 310K and equilibrated for 200 ps (NVT) with backbone constraints. The 10 ns NPT simulation (T = 310 K, P = 1 atm) with backbone constraints was used to equilibrate the system. Unlike the simulation of peptide aggregation in solution, we chose a temperature of 310 K in the simulations of peptides with the membrane. This is because at high temperature (400 K), area per lipid of the membrane is much larger than that of 310 K, thus we avoid membrane disruption at lower simulation temperatures. In the simulation with the membrane, the cut-offs for VDW and electrostatic interactions were set to 1.2 nm. Unbiased simulation was carried out for 150 ns. The aggregate quickly attached to the membrane during the simulation. Steered MD simulation was then carried out with the 50 ns snapshot. The last guanine unit in the N-terminal closest to the membrane was pulled along the z-axis, using a spring constant of 3000 kJ mol/nm^2 and a pulling velocity of 0.1 nm/ns.

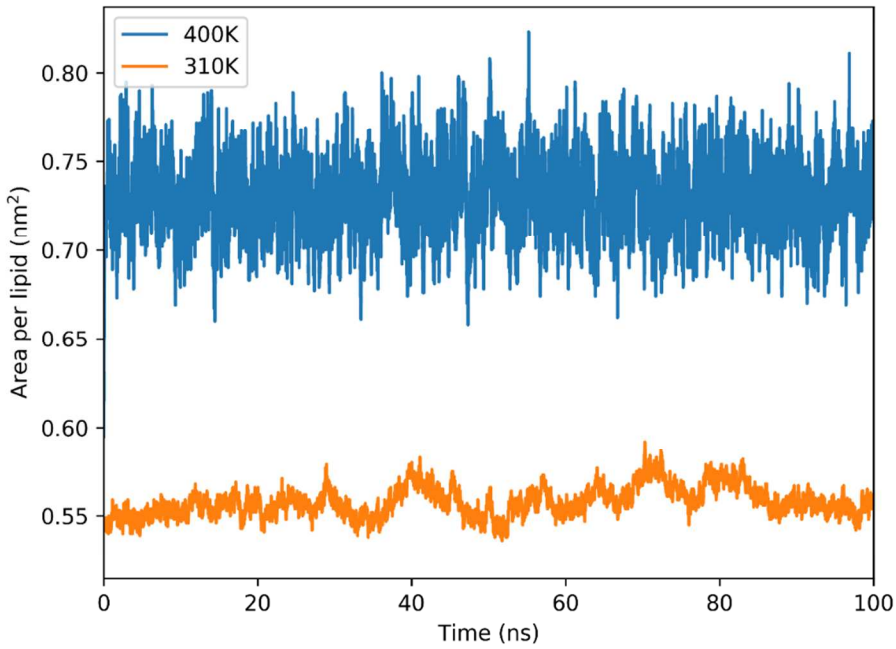

Figure S10. Time evolution of the area per lipid of the membrane at 310 K (orange line) and 400 K (blue line).

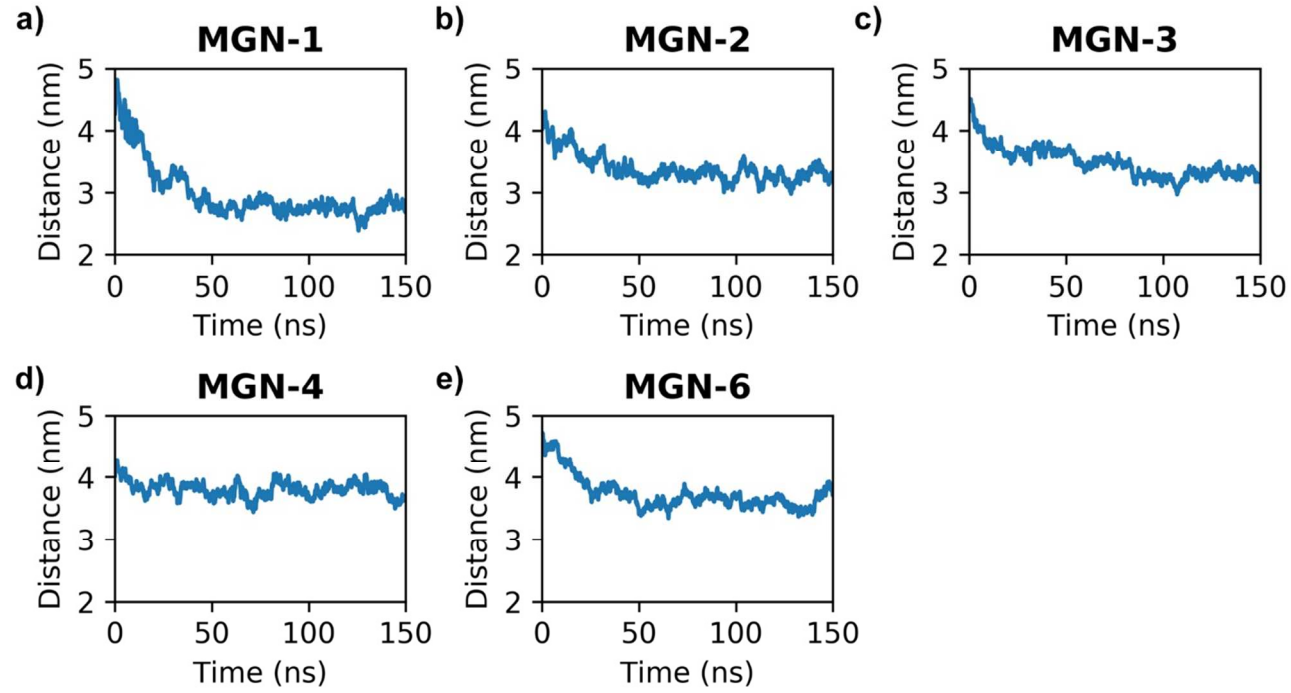

Figure S11. a-e) Time evolution of the z-distance between the COM of peptide aggregates and the COM of the membrane. Z-distance is denoted as the direction perpendicular to membrane surface.

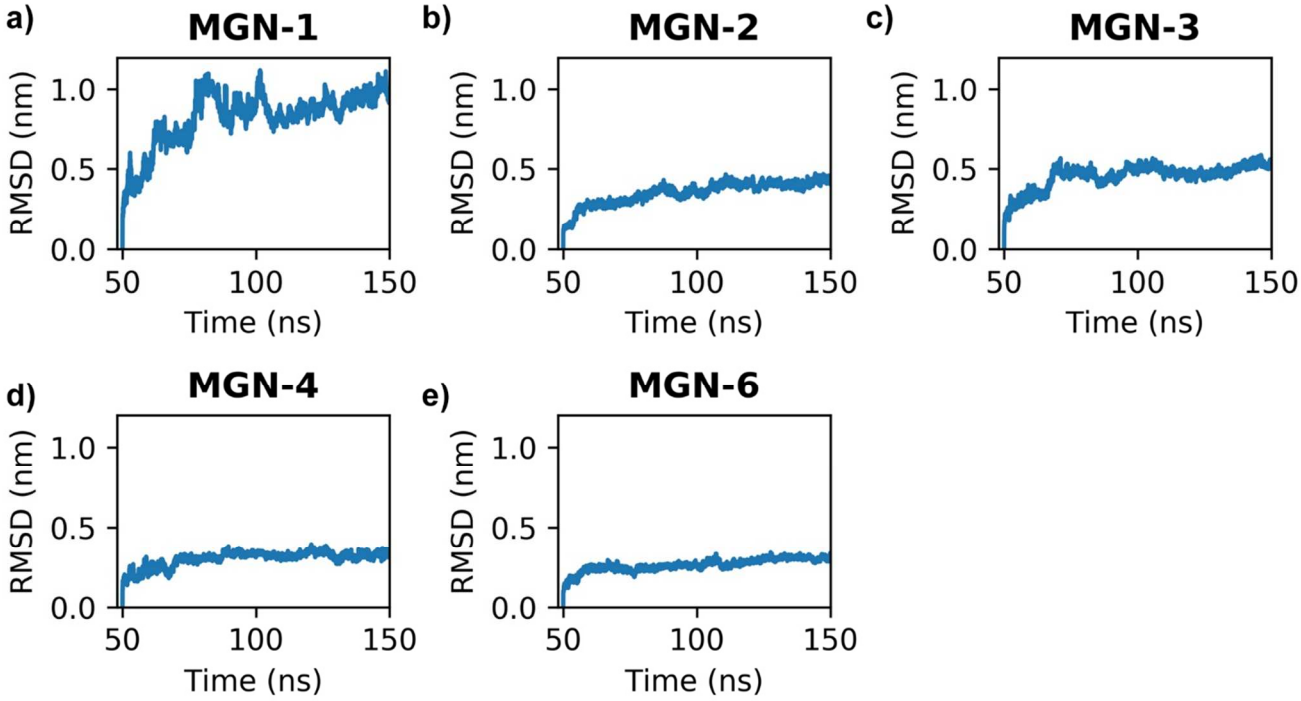

Figure S12. a-e) Time evolution of the RMSD values of the peptide aggregates on the membrane, whereby the structure of the peptide aggregate at 50 ns was taken as a reference.

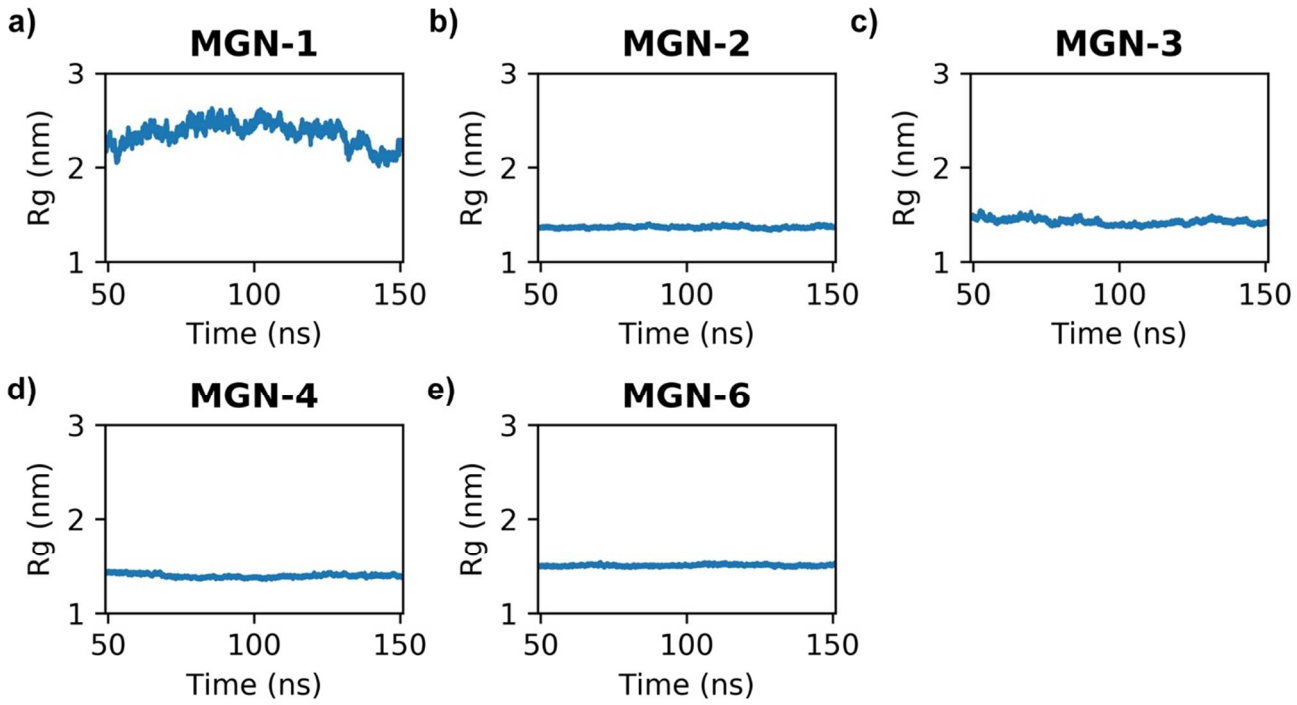

Figure S13. a-e) Radius of gyration (Rg) changes of the peptide aggregates on the membrane for the 50 – 150 ns simulation time-frame.

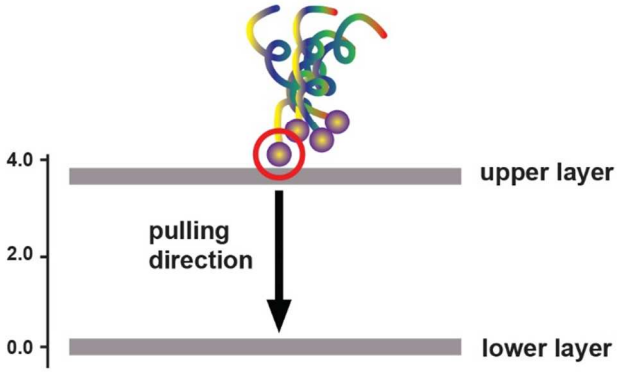

Figure S14. Pulling direction and guanine unit (circled red) on which the pulling force is applied. Purple spheres represent the N-terminal guanine unit.

The COM space between the pulled guanine unit and the low-layer membrane along the z-axis was 0.1 nm for each window, generating 37 windows for the umbrella sampling simulation. Each window was simulated for 50 ns. The permeation Gibbs free energy was calculated using the weighted histogram analysis method (WHAM)[4] according to equations (2) and (3):

$$\mathrm{P}(x) = \frac{\sum_{i=1}^{N_{sims}} n_i(x)}{\sum_{i=1}^{N_{sims}} N_i e^{\left(\frac{F_i - U_{bias,i}(x)}{k_B T}\right)}} \qquad (2)$$

$$F_i = -k_B T ln\left(\sum_{x_{bins}} P(x)\, e^{\frac{-U_{bias,i}(x)}{k_B T}}\right) \qquad (3)$$

Where N_{sims} is the number of simulations, $n_i(x)$ is the number of counts associated with x, $U_{bias,i}$ and F_i are the biasing potential and free energy shift from the simulation I, P(x) is the best estimate of the unbiased probability distribution, k_B and T are the Boltzmann constant and simulation temperature, P(x) and F_i are unknowns and solved by iteration to self-consistency.

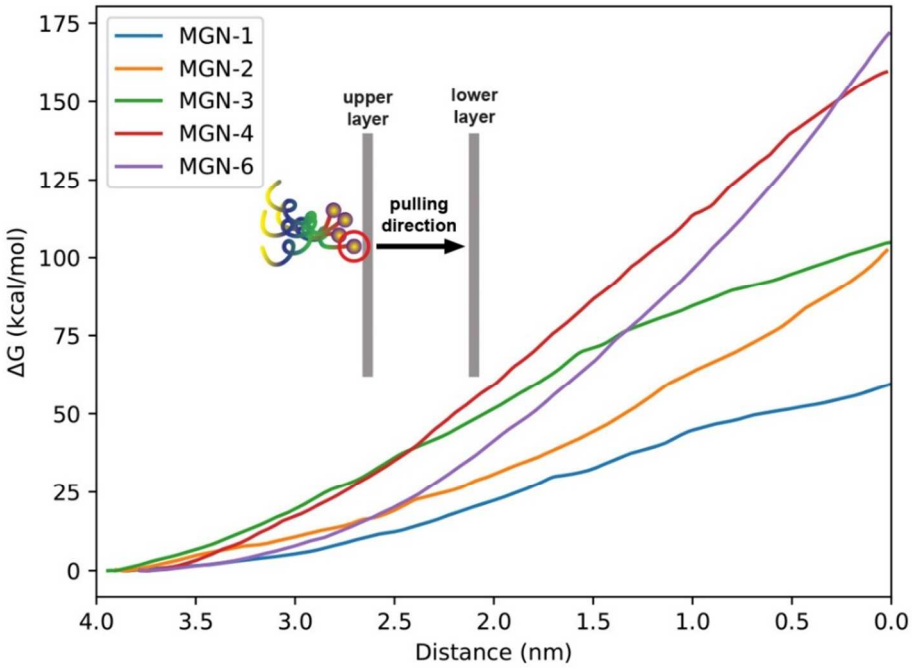

Figure S15. Change of the potential of mean forces with respect to the pulling direction distance. Insert: pulling direction of the SMD/umbrella sampling simulation.

Histogram analysis of our umbrella sampling simulations was performed to measure overlap between adjacent windows. As shown in Figure S15, we show sufficient overlap between adjacent windows, confirming the validity of our umbrella sampling simulations.

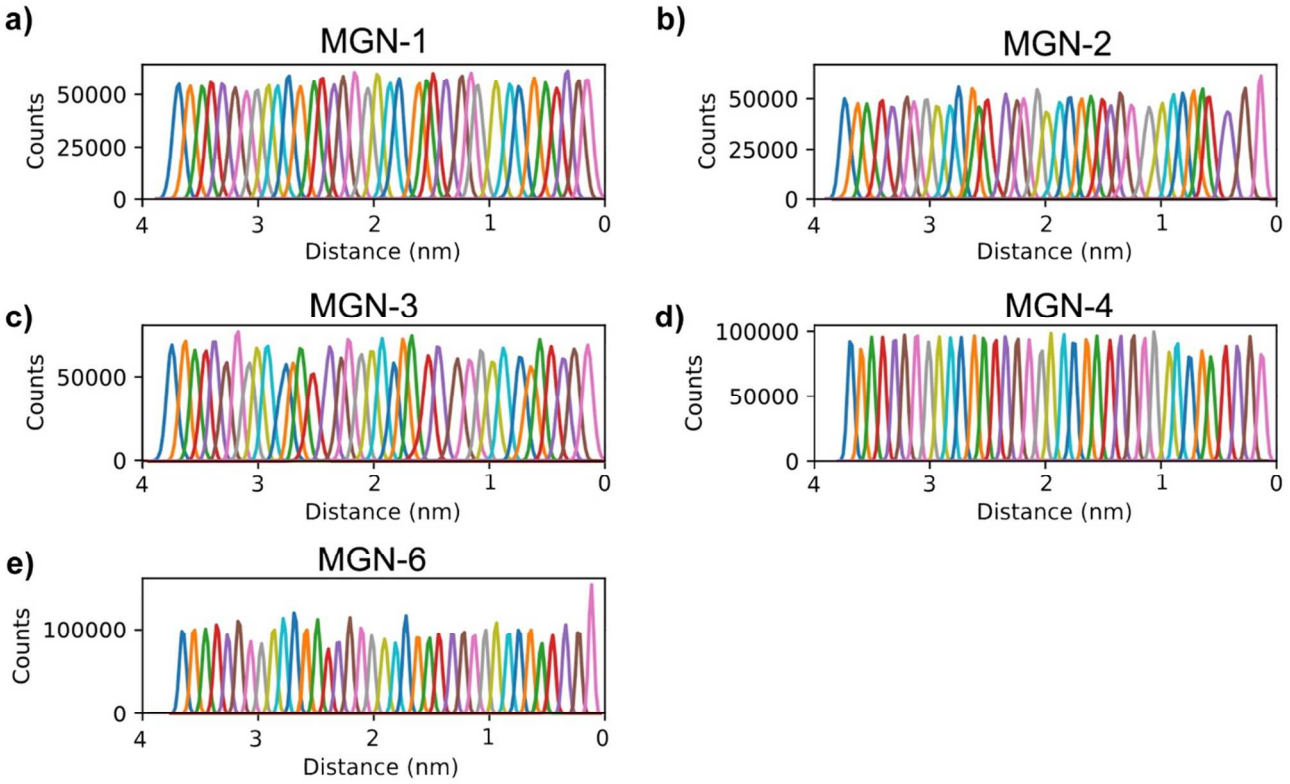

Figure S16. Histogram analysis of the umbrella sampling simulations.

All structures pertinent to our MD simulations were produced with VMD.[5]

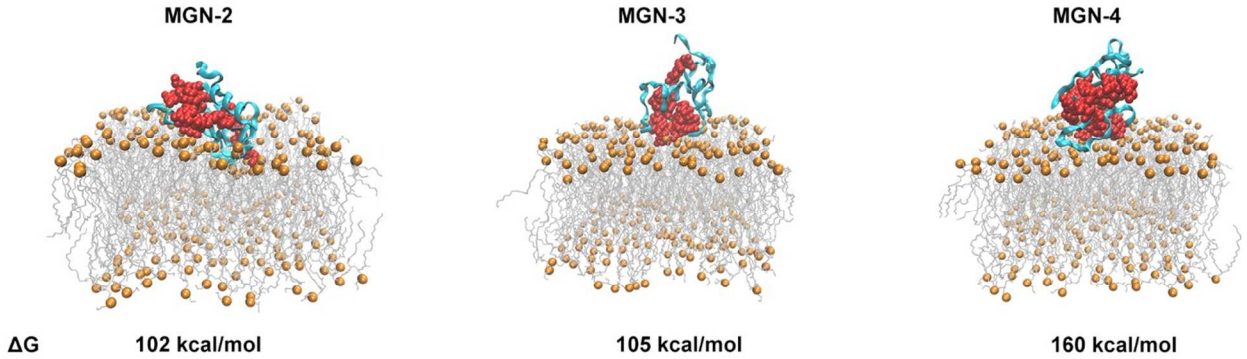

Figure S17. Permeation Gibbs free energy of MGN-2, MGN-3 and MGN-6. Final snapshots of MGNs aggregates attached to the membrane. The MGN II peptide scaffold is colored cyan, guanine units are colored red, and lipids are colored orange and grey.

Table S6. The synthesis and analysis of CAM-1.

CAM-1: Yield 10.9%, purity HPLC 98.6%, MALDI-TOF (m/z): calcd for 2060.29, found $[M+H]^+$ 2061.50.
Guanine -KWKLFKKIGAVLKVL-NH_2

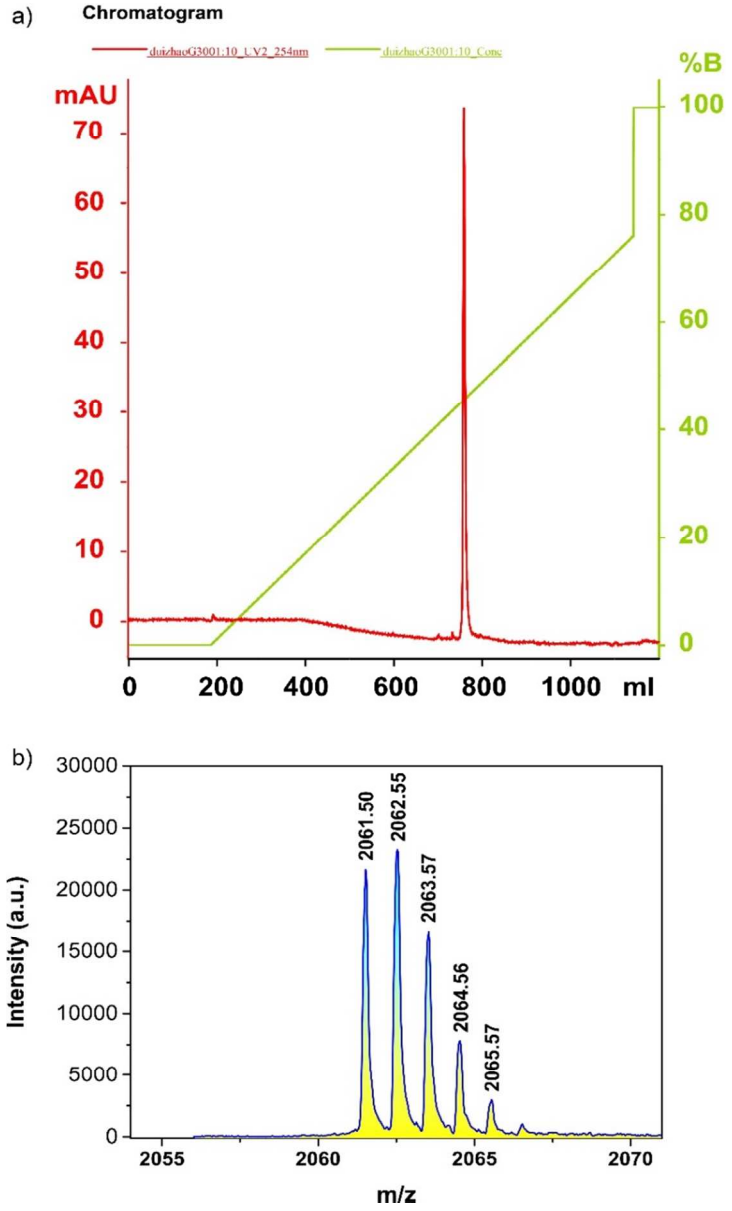

Figure S18. (a) HPLC analysis report and (b) M-TOF of CAM-1.

Table S7. The synthesis and analysis of CAM-6.

CAM-6: Yield 6.5%, purity HPLC 99.2%, MALDI-TOF (m/z): calcd for 3515.83, found $[M+H]^+$ 3516.43.
Guanine Guanine Guanin Guanine Guanine Guanine -KWKLFKKIGAVLKVL-NH_2

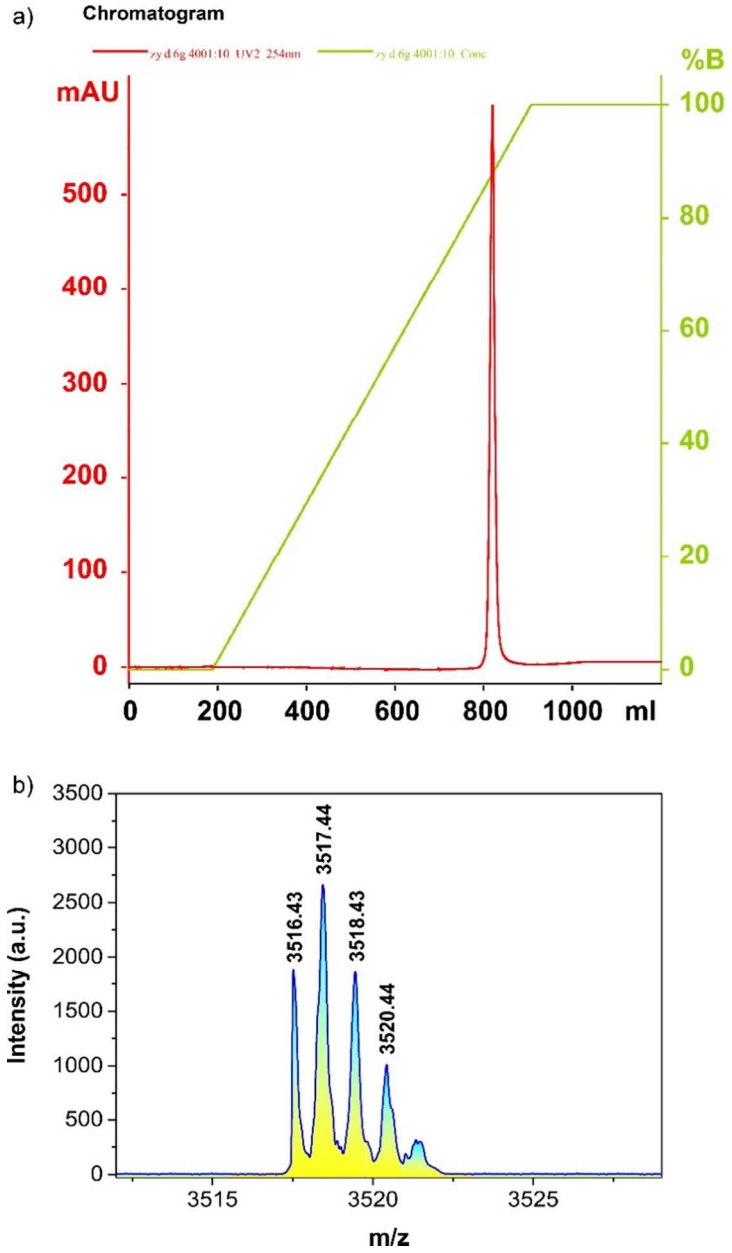

Figure S19. (a) HPLC analysis report and (b) M-TOF of CAM-6.

REFERENCES

(1) Jackson, M., Mantsch, H. H., and Spencer, J. H. (1992) *Biochemistry 31*, 7289–7293.
(2) Gregory, S. M., Pokorny, A., and Almeida, P. F. F. (2009) *Biophys. J. 96*, 116–131.
(3) Jo, S., Cheng, X., Lee, J., Kim, S., Park, S.-J., Patel, D. S., Beaven, A. H., Lee, K. I., Rui, H., Park, S., Lee, H. S., Roux, B., MacKerell, A. D., Klauda, J. B., Qi, Y., and Im, W. (2017) *J. Comput. Chem. 38*, 1114–1124.
(4) Kumar, S., Rosenberg, J. M., Bouzida, D., Swendsen, R. H., and Kollman, P. A. (1992) *J. Comput. Chem. 13*, 1011–1021.
(5) Humphrey, W., Dalke, A., and Schulten, K. (1996) *J. Mol. Graph. 14*, 33–38, 27–28.